Pharm Res (2013) 30:826–835
DOI 10.1007/s11095-012-0923-1

RESEARCH PAPER

# Rapid Insight into Heating-Induced Phase Transformations in the Solid State of the Calcium Salt of Atorvastatin Using Multivariate Data Analysis

Niels Peter Aae Christensen • Bernard Van Eerdenbrugh • Kaho Kwok • Lynne S. Taylor • Andrew D. Bond • Thomas Rades • Jukka Rantanen • Claus Cornett

Received: 24 August 2012 / Accepted: 22 October 2012 / Published online: 10 November 2012


## ABSTRACT

***Purpose*** To investigate the heating-induced dehydration and melting behavior of the trihydrate phase of the calcium salt of atorvastatin.

***Methods*** Multivariate curve resolution (MCR) was used to decompose a variable-temperature synchrotron X-ray powder diffraction (VT-XRPD) data matrix into diffraction patterns and concentration profiles of pure drug phases.

***Results*** By means of the MCR-estimated diffraction patterns and concentration profiles, the trihydrate phase of the drug salt was found to dehydrate sequentially into two partially dehydrated hydrate structures upon heating from 25 to 110°C, with no associated breakage of the original crystal lattice. During heating from 110 to 140°C, the remaining water was lost from the solid drug salt, which instantly collapsed into a liquid crystalline phase. An isotropic melt was formed above 155°C. Thermogravimetric analysis, hot-stage polarized light microscopy, and hot-stage Raman spectroscopy combined with principal component analysis (PCA) was shown to provide consistent results.

***Conclusions*** This study demonstrates that MCR combined with VT-XRPD is a powerful tool for rapid interpretation of complex dehydration behavior of drug hydrates, and it is also the first report on a liquid crystalline phase of the calcium salt of atorvastatin.

**KEY WORDS** calcium atorvastatin · multivariate data analysis · phase transformation · Raman spectroscopy · synchrotron XRPD

## INTRODUCTION

40% of new chemical entities entering clinical trials fail to become drug products due to patent concerns and issues like solubility and drug interactions (1). In order to minimize the associated costs, the physical forms of drug candidates, and transformations among them, must be identified, understood and optimized for *in vivo* performance, manufacture of high-quality products and protection of intellectual property rights.

Water has the ability to associate with certain solids to form crystal hydrates, which possess different physicochemical and mechanical properties than the corresponding anhydrous solids (2,3). For pharmaceutical compounds, transformations between hydrate and anhydrous forms may occur during high-shear wet granulation and drying of powders in manufacturing processes (4–6). Dehydration of hydrate crystals has been reported to happen by either

**Electronic supplementary material** The online version of this article (doi:10.1007/s11095-012-0923-1) contains supplementary material, which is available to authorized users.

N. P. A. Christensen · T. Rades · J. Rantanen · C. Cornett (✉)
Department of Pharmacy, Faculty of Health and Medical Sciences
University of Copenhagen
Copenhagen, Denmark
e-mail: claus.cornett@sund.ku.dk

B. Van Eerdenbrugh · K. Kwok · L. S. Taylor
Department of Industrial and Physical Pharmacy, College of Pharmacy
Purdue University
West Lafayette, Indiana, USA

A. D. Bond
Department of Physics, Chemistry and Pharmacy
University of Southern Denmark
Odense, Denmark

B. Van Eerdenbrugh
Laboratory for Pharmacotechnology and Biopharmacy
Katholieke Universiteit Leuven
Leuven, Belgium

breakage of the crystal lattice, followed by formation of a new crystal lattice for the anhydrous form, or by retaining the original hydrate crystal lattice during and after dehydration. The latter class of dehydrations leads to formation of high-energy dehydrated-hydrate structures, which can be relieved through either incorporation of small molecules into the lattice (resolvation, *i.e.* these structures are highly hygroscopic) or by structural relaxation (7).

Dehydration mechanisms of hydrate-forming drugs are commonly studied by variable-temperature X-ray powder diffraction (VT-XRPD), vibrational spectroscopy and more traditional thermal methods (8–12). When it comes to identifying, understanding and predicting the dehydration behavior of higher hydrates, several solid phases may be encountered during dehydration. This complicates the qualitative and quantitative assessment of the transformation kinetics (13,14). Moreover, since some solid forms encountered may be metastable, it is not always possible to isolate reference material for calibration samples. For XRPD analyses, this can prevent determination of crystal structures of individual phases in a complex mixture, which greatly complicates or hinders any quantitative phase analysis. In such cases, variable-temperature XRPD in combination with multivariate curve resolution (MCR) may have a potential for rapid in-depth assessment of phase transformations encountered on heating, since MCR offers calibration-free estimation of pure analyte signals (*e.g.* X-ray powder diffraction patterns or spectral profiles) and concentration profiles from multivariate data matrices. In other words, MCR may facilitate quantification of complex mixtures and even isolation of XRPD patterns for pure phases when no prior information is available about the structure of those phases.

MCR methodology assumes that data fit to the following model:

$$\mathbf{D} = \mathbf{C}\mathbf{S}^{\mathbf{T}} + \mathbf{E}$$

where $\mathbf{D}$ is the data matrix, $\mathbf{C}$ contains the concentration profiles of the pure components, $\mathbf{S}^{\mathbf{T}}$ contains the transposed signals of the pure components and $\mathbf{E}$ contains the residual error (Fig. 1). In the specific case of monitoring structural changes by XRPD, $\mathbf{D}$ represents the measured XRPD patterns which are expected to be mixtures, and $\mathbf{S}$ represents the patterns of the pure components (as of yet unknown). When applying MCR, the number of physical or chemical components encountered in the data matrix should be resolved by *e.g.* principal component analysis (PCA) or evolving factor analysis. In many chemical/pharmaceutical problems, the expected number of constituent phases may already be known from other techniques (*e.g.* thermogravimetric analysis in the case of hydrates). After determining the number of components, an initial guess of the pure signal profiles ($\mathbf{s_1}$, $\mathbf{s_2}$, *etc.*) must be provided before the concentration profiles ($\mathbf{c_1}$, $\mathbf{c_2}$, *etc.*) can be estimated, or *vice versa*. These could be obtained, for example, by taking representative patterns from clusters obtained from principal component analysis (PCA) (15). Next, the predicted signals and concentration profiles can be refined by applying constraints such as non-negativity (for estimated signal and concentration profiles) and sum to unit concentration by an alternating least-squares approach for minimizing the residual error $\mathbf{E}$ (16,17). The result should be a set of pure signals for the components in the mixture (*i.e.* a set of XRPD patterns for the pure phases). In recent years, the use of MCR has been described for a variety of purposes such as near-infrared chemical imaging of pharmaceutical tablets and analysis of counterfeit drug products by Raman microscopy (18,19). To the best of our knowledge, however, the procedure has not been applied to XRPD patterns describing complex phase transformations.

The aim of the present study was to investigate heating-induced solid-state changes encountered during dehydration and melting of the trihydrate of the calcium salt of atorvastatin (THCaA, Fig. 2) with a focus on increasing the understanding of the physical instability of hydrate forming drugs at elevated temperatures in typical pharmaceutical manufacturing environments. The THCaA system is a prime candidate for the MCR approach on VT-XRPD data, because crystal structures have not so far been reported for any of the hydrate or anhydrous phases. Synchrotron XRPD data have previously been reported for THCaA, from which a unit cell has been deduced by Pawley refinement (20,21). However, full structural information has not been established. Here, we use MCR to decode the information in a variable-temperature XRPD data matrix and show that this approach can provide a rapid interpretation of complex dehydration behavior, even in the absence of detailed structural knowledge. Moreover, there is currently a trend towards continuous manufacturing of solid dosage pharmaceuticals in the pharmaceutical industry, which requires effective and inexpensive in-line process monitoring and control of the continuous manufacturing processes. In this context, in-line vibrational spectroscopy offers effective in-process evaluation of quality attributes of solid dosage pharmaceuticals during manufacturing (22). In order to illustrate the potential use of Raman spectroscopy, it was thus decided also to investigate the degree of consistency between the MCR approach on VT-XRPD data and results established by Raman spectroscopy and PCA.

## MATERIALS AND METHODS

The trihydrate of the calcium salt of atorvastatin (Ca$(C_{33}H_{34}FN_2O_5)_2 \cdot 3H_2O$; THCaA) was purchased from AvaChem Scientific (San Antonio, TX, USA) and assessed by

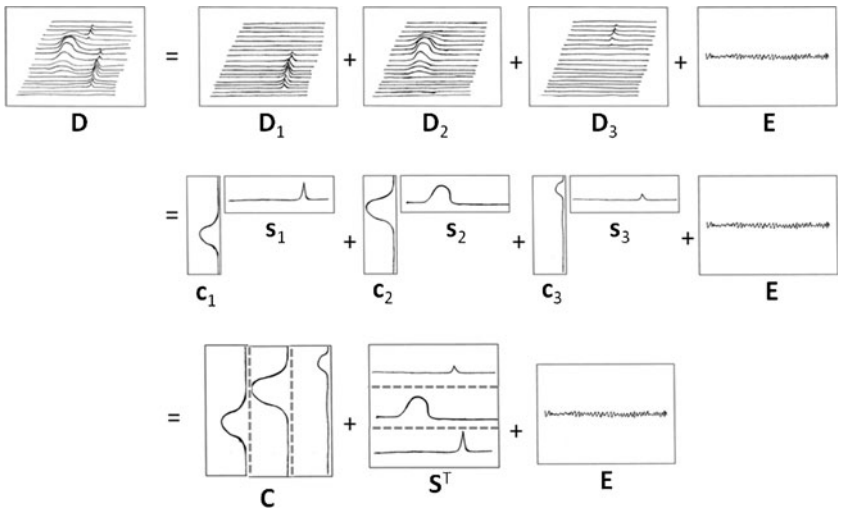


**Fig. 1** Schematic representation of multivariate curve resolution of a three-component system, where **D** is a data matrix, **C** contains the concentration profiles, $\mathbf{S}^{\mathbf{T}}$ contains the transposed signal profiles and **E** contains the residual error. $\mathbf{D_1}$-$\mathbf{D_3}$, $\mathbf{c_1}$-$\mathbf{c_3}$ and $\mathbf{s_1}$-$\mathbf{s_3}$ are the data matrices, concentration profiles, and signal profiles of component 1–3, respectively.

laboratory X-ray powder diffraction (XRPD) to be identical to the solid phase referred to in the literature as Form I (23).

### Thermogravimetric Analysis

Thermogravimetric analysis (TGA) was performed using a Perkin Elmer TGA7 (Perkin Elmer, Norwalk, CT, USA) controlled by Pyris software version 7.0 (Perkin Elmer, Norwalk, CT, USA). A ferromagnetic standard and a 100 mg standard weight were used for temperature and weight calibration, respectively. Samples were analyzed in triplicate in a flame-cleansed open aluminum pan heated at 1°C/min and 10°C/min from 25 to 200°C under nitrogen flow.

### Differential Scanning Calorimetry

Differential scanning calorimetry (DSC) was performed using a Perkin Elmer Diamond DSC (Perkin Elmer, Norwalk, CT, USA) equipped with an Intracooler 2P (Ultra Low Special Products BV, Ede, The Netherlands) and controlled by Pyris software version 7.0 (Perkin Elmer, Norwalk, CT, USA). Samples were analyzed in open aluminum pans. Indium and tin were used for temperature and heat flow calibration, respectively, and samples were analyzed in triplicate from 25 to 200°C at 1°C/min and 10°C/min under nitrogen flow.

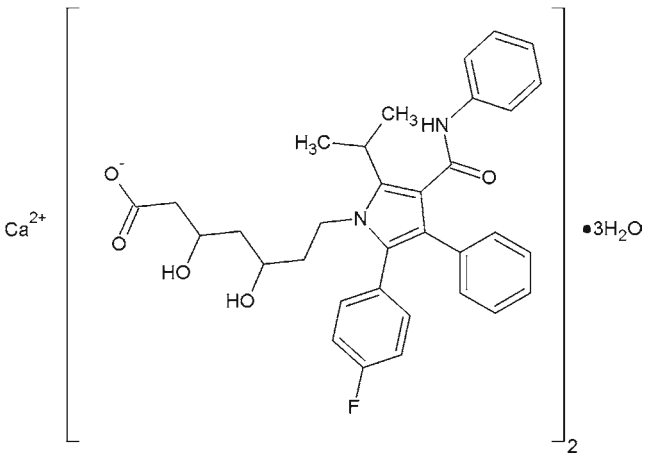


**Fig. 2** Chemical structure of the trihydrate phase of the calcium salt of atorvastatin (THCaA).

### Hot-Stage Polarized Light Microscopy

A Zeiss Axiolab microscope (Carl Zeiss Inc., Oberkochen, Germany) coupled with a Mettler-Toledo FP90 Central Processor, a Mettler-Toledo FP82HT hot-stage (Mettler-Toledo, Greifensee, Switzerland) and a Moticam 10 10.0 megapixel digital camera (Motic Co. Ltd., Xiamen, China) was used for hot-stage cross-polarized light microscopy. Samples were placed on a glass slide in the hot stage and were allowed to equilibrate for 5 min at the selected temperature prior to image acquisition. No oil was used for the microscopy samples.

### Variable-Temperature X-ray Powder Diffraction

Time-resolved X-ray powder diffraction (XRPD) experiments were conducted at the Advanced Photon Source beam station 12-ID-B (Argonne National Laboratories, Argonne, IL, USA). The simultaneous Small-Angle X-ray Scattering/Wide-Angle X-ray Scattering (SAXS/WAXS) instrument was equipped with Pilatus 2 M (SAXS) and 300 K (WAXS) detectors (Dectris Ltd., Baden, Switzerland). The energy of the X-ray source was 12 keV ($\lambda = 1.033$ Å), and the sample to detector distances were ca. 2.2 m (SAXS) and 0.45 m (WAXS). The $Q$ range was 0.005–0.76 $Å^{-1}$ for SAXS and 0.88–2.44 $Å^{-1}$ for WAXS. The SAXS and WAXS ranges were calibrated using silver behenate and

the absolute intensity was calibrated using glassy carbon. The crystalline sample was prepared in an aluminum DSC pan (Tzero DSC sample pans, TA Instruments, New Castle, DE, USA) and subjected to a temperature ramp using a Linkam DSC600 stage controlled by a Linkam CI-93 temperature program (Linkam Scientific Instruments Ltd., Surrey, United Kingdom). The sample was heated from room temperature to 168°C using a heating rate of 1°C per minute and the sample was measured once every minute using an exposure time of 1 s. The synchrotron X-ray powder diffractometer allows for exceptionally fast acquisition of high-quality data whereby rapid dehydration events can be captured. The diffraction data are presented using the wavelength-independent unit $Q(= 2\pi/d$-spacing, unit $Å^{-1})$. Representative patterns plotted using units of $2\theta$ (°) for CuKα radiation are included as Supplementary Material I and II.

### Hot-Stage Raman Spectroscopy

Raman spectra were collected using a Raman RxN2 Hybrid equipped with a PhAT System probe head with a 250 mm working distance and 6 mm spot size (Kaiser Optical Systems Inc, Ann Arbor, MI, USA). Laser power and wavelength were 400 mW and 785 nm, respectively. Samples were placed in a THMS600 hot stage, controlled by a THMS93 controller (Linkam Scientific Instruments LTD, Waterfield, United Kingdom) and heated at 1°C/min from 25 to 170°C. Raman spectral data in the spectral range 150–1890 $cm^{-1}$ was collected in-line in 1 min intervals and each collected spectrum was the average of 5 accumulations with a 5 s exposure time each. Invictus Laser Control software version 1.4.0 (Kaiser Optical Systems Inc., Ann Arbor, MI, USA) was used for controlling the laser and iC Raman version 4.1.910 (Kaiser Optical Systems Inc., Ann Arbor, MI, USA) was used for data collection.

### Multivariate Statistical Modeling of X-ray Powder Diffraction Patterns and Raman Spectral Profiles

MatLab version 7.9.0 (R2009b, MatWorks Inc., Natick, MA, USA) and PLS_Toolbox version 6.2 (Eigenvector Research, Manson, WA, USA) were used for performing principal component analysis (PCA) on the Raman spectral data. Principal component analysis (PCA) allows for identification of patterns in multivariate data sets by reducing the original multiple variables (wavelengths in case of spectral data) into fewer new orthogonal variables describing as much of the variability in the data as possible. These new pseudo variables are called principal components. Trends in the data can be visualized by the scores and loadings of the data points in the principal component space, where the scores describe the location of the data points in the principal component space, and the loadings describe the relationship between the original data space and the principal component space. The Raman data were preprocessed by standard normal variate correction and mean centering prior to PCA (15,24).

Multivariate curve resolution (MCR) on the variable-temperature XRPD data matrix was performed using the MCR-ALS Toolbox (available for free at www.mcrals.info) for MatLab as described by Jaumot *et al.* (25). No data preprocessing was applied before MCR.

## RESULTS AND DISCUSSION

### Thermogravimetric Analysis and Differential Scanning Calorimetry

The starting material ($Ca(C_{33}H_{34}FN_2O_5)_2 \cdot 3H_2O$; THCaA) shows stepwise dehydration by thermogravimetric analysis (TGA, Fig. 3) and differential scanning calorimetry (DSC, included as Supplementary Material III), with onset temperatures of phase transformations at approximately 55°C, 105°C, 125°C and 155°C. The weight loss in each dehydration step corresponds to expectations, since the weight of one water molecule ($M_w$ 18 g/mol) corresponds to 1.49% of the weight of THCaA ($M_w$ 1209 g/mol). Hence, solid phases containing three (THCaA), two (DHCaA), one (MHCaA) and zero (AHCaA) moles of water per one mole of calcium ions, and a molten phase are anticipated between 30 and 55°C, 75 and 105°C, 115 and 125°C, 135 and 155°C, and above 155°C, respectively, when heating at 1°C per minute.

### Hot-Stage Polarized Light Microscopy

Upon heating THCaA from 30 to 140°C, no visual change was detected by polarized light microscopy. Squeezing the material between a glass slide and cover slip at 140°C, however, induced changes in the appearance of the material, since the drug compound takes on a viscous and birefringent nature at this temperature (included as Supplementary Material IV). Dehydration of calcium salts has previously been associated with formation of liquid crystalline phases, where the liquid crystalline state is an intermediate between the crystal and the melt, with long-range order existing in only one or two dimensions (26–31). To the best of our knowledge, this is the first report indicating a liquid crystalline phase of the calcium salt of atorvastatin. Upon heating from 155 to 165°C, the observed birefringence fades away as an isotropic melt is formed. The liquid crystalline phase could also be observed upon repeated heating and cooling of the drug salt between 100 and 175°C, and brown banana-shaped silhouettes occasionally appeared in the liquid crystalline material (Fig. 4).

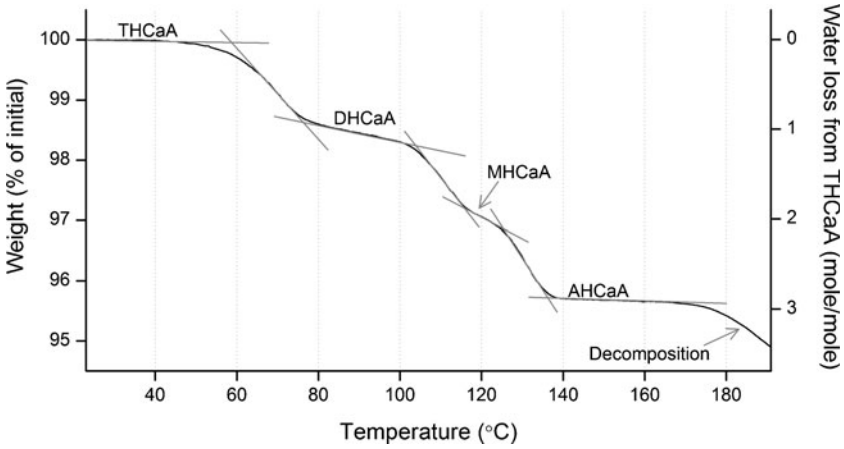


**Fig. 3** Thermogravimetric analysis of the trihydrate phase of the calcium salt of atorvastatin (THCaA) heated at 1°C per minute. Phases containing three (THCaA), two (DHCaA), one (MHCaA) and zero (AHCaA) moles of water per one mole of calcium ions are indicated in the thermogram.

## Variable-Temperature X-ray Powder Diffraction

Variable-temperature X-ray powder diffraction (XRPD) patterns were collected between 18 and 168°C at 1°C intervals (Fig. 5). From the TGA data (Fig. 3), this temperature range is expected to encompass several dehydration events. The small-angle X-ray scattering (SAXS) region of the initial trihydrate phase contains five well-resolved isolated peaks that correspond to the (001), (002), (003), (011) and (010) reflections in the triclinic unit cell reported by Antonio *et al.* (a = 5.453, b = 9.885, c = 30.264 Å, α = 76.85, β = 99.12, γ = 105.31°) (20). The unit-cell parameters are consistent with an expected laminar structure. The wide-angle X-ray scattering (WAXS) region contains much broader overlapping peaks, and attempted Pawley refinement of this region, using the established unit cell as a starting point, gave fits of only poor quality ($\chi^2$ ca 15). Thus, the principal structural features that can be extracted reliably from the data are d(001) and d(010), which are plotted in Fig. 6. The peaks in the SAXS region thus provide a clear measure of the laminar spacing (*i.e.* d(001)) and a shorter spacing (*i.e.* d (010)) within the layers of the solid drug compound, but no reliable information on shorter distances.

Upon heating up to 135°C, no abrupt changes are observed in the diffraction patterns, indicating that the crystal lattice of the trihydrate phase remains ostensibly intact during dehydration of the first two moles of water molecules. The laminar spacing (*i.e.* d(001)) shows thermal expansion of ca. 0.4 Å over this temperature range, with a subtle sigmoidal shape visible between 60 and 120°C, with an inflection point near 80°C. In the same temperature range, d(010) shows a more clear sigmoidal curve, with the dimension contracting overall by approximately 0.1 Å. In this case, the end of the sigmoidal region is reached clearly at 100°C, prior to the second dehydration observed in the TGA. Thus, it appears that the first dehydration causes a

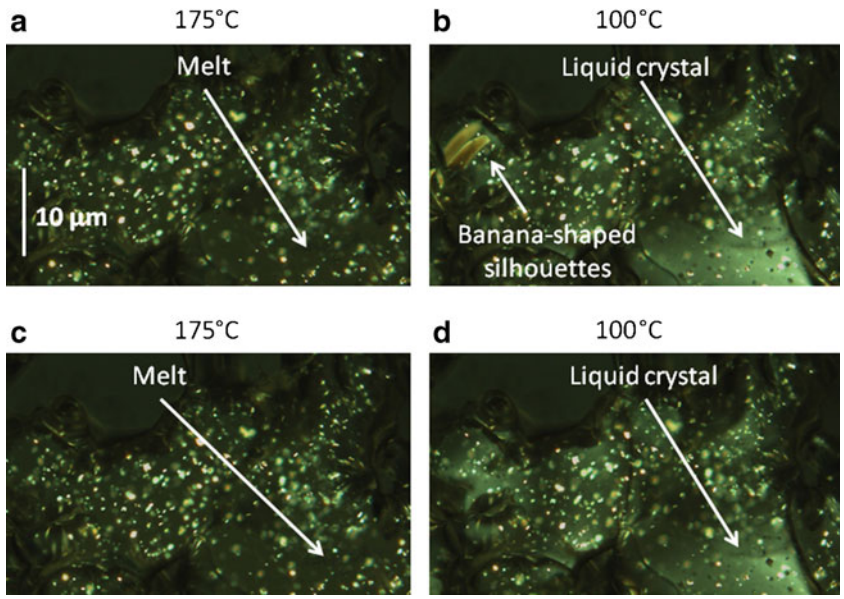


**Fig. 4** Hot-stage polarized light microscopy of the calcium salt of atorvastatin during sequential heating and cooling to (**a**) 175°C, (**b**) 100°C, (**c**) 175°C and (**d**) 100°C. The majority of the material appears molten at 175°C, whereas a birefringent phase becomes visible upon cooling to 100°C. Banana-shaped silhouettes are visible in the left side of (**b**).

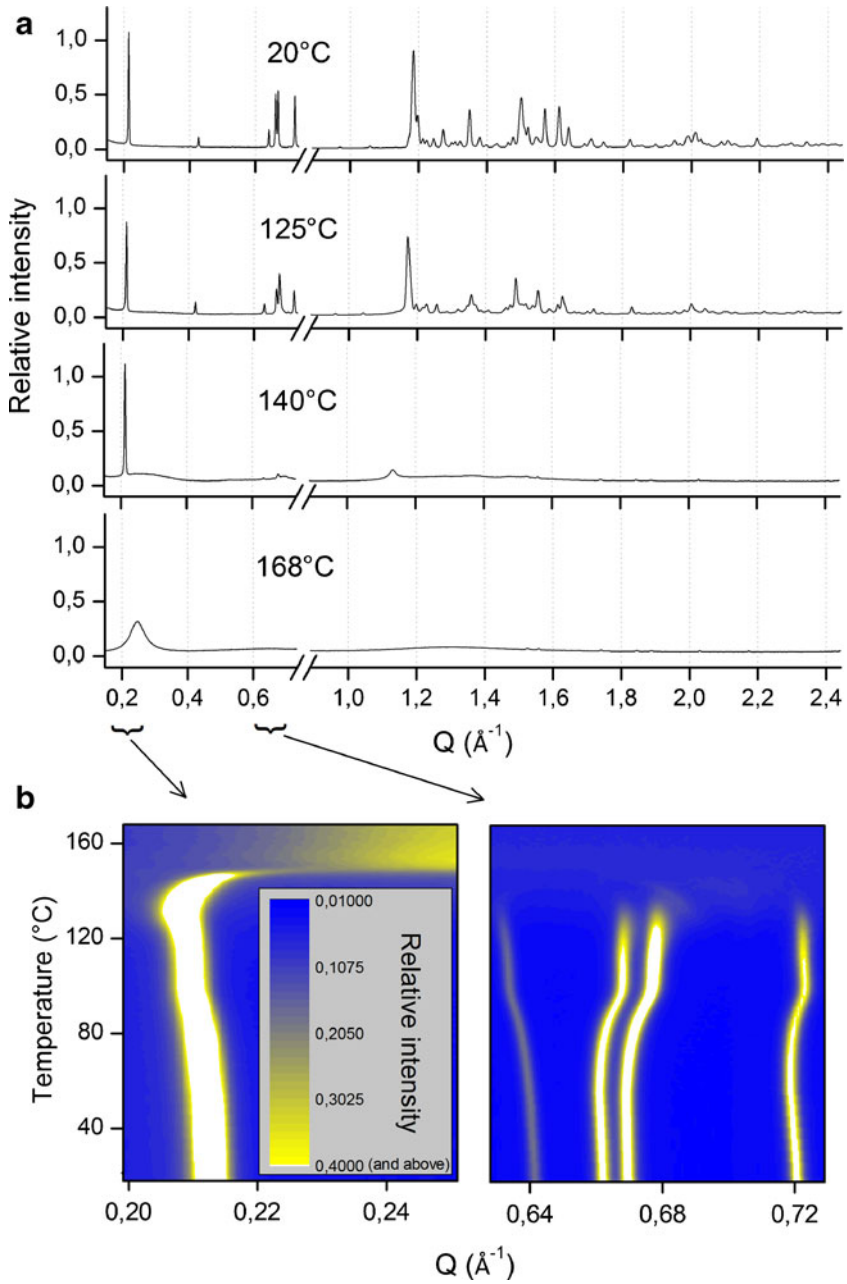


**Fig. 5** (**a**) Combined experimentally obtained variable-temperature small-angle (0.148 to 0.734 $Å^{-1}$) and wide-angle (0.888 to 2.442 $Å^{-1}$) XRPD patterns of the calcium salt of atorvastatin. (**b**) *Contour plot* showing effect of temperature on selected diffraction peaks.

significant contraction within the laminar structure, while the second dehydration has a less abrupt effect.

Upon further heating above 135°C, the majority of diffraction peaks vanish, while d(001) remains clear at Q = 0.21 $Å^{-1}$ and a new broad peak appears at Q ≈ 1.14 $Å^{-1}$. This is consistent with the formation of a liquid crystal phase, since it indicates that the long-range order of the solid phase is diminished. The persistence of the observed diffraction peak at Q = 0.21 $Å^{-1}$ ($d$ = 29.9 Å) demonstrates that the liquid crystalline phase retains a laminar structure similar to that which must be present in the solid. To date, the exact nature of the laminar structure has not been established. Upon heating to 155°C, all diffraction peaks vanish due to melting of the material. A broad peak at Q ≈ 0.25 $Å^{-1}$, present between 155 and 168°C, indicates that some degree of short-range order could be maintained in the melt up to this temperature. After return to ambient conditions, the drug compound was XRPD amorphous (data not shown).

## Multivariate Curve Resolution

The difficulties associated with Pawley refinement for the mixed phases prohibit reliable assessment of the peak intensities for the individual phases, which prevents any quantitative phase analysis by conventional means. Thus, the

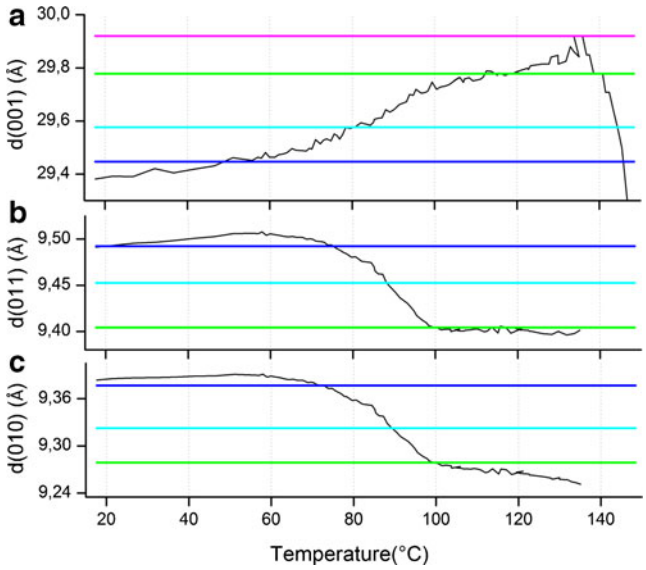


**Fig. 6** Temperature effect on (**a**) d(001), (**b**) d(011) and (**c**) d(010) of the calcium salt of atorvastatin derived from the positions of the isolated peaks in the small-angle XRPD region during dehydration of the trihydrate phase of the calcium salt of atorvastatin (THCaA). The *horizontal lines* indicate the values taken from the XRPD patterns estimated by MCR analysis (see text and Fig. 8) for the first (*i.e.* THCaA, *blue*), second (DHCaA, *cyan*), third (MHCaA, *green*) and fourth form (AHCaA, *magenta*) encountered during dehydration.

multivariate curve resolution (MCR) approach was applied. Initially, the complete variable-temperature XRPD data matrix was established to contain contributions from five components (THCaA, DHCaA, MHCaA, the liquid crystalline phase and melt) by principal component analysis (not shown). This result is clearly consistent with the prior knowledge from the TGA and DSC experiments. Accordingly, an MCR model based on five pure components was used to decompose the data matrix. The first MCR model was built with no constraints on the alternating least-squares algorithm, and the initial estimates of pure signal profiles were selected as the experimentally obtained diffraction patterns at 50°C, 85°C, 115°C, 137°C and 155°C. With this model, MCR predicts the concentrations of individual phases to become negative in some temperature intervals, and the initial trihydrate phase (THCaA) and the first dehydrated structure (DHCaA) are predicted to reappear in the data between 140 and 150°C (Fig. 7). This is clearly inconsistent with prior knowledge and physical expectations.

To improve the MCR model, the alternating least-squares algorithm was constrained to non-negativity on estimated concentration and signal profiles, and equality constraints were used to guide the predicted concentration profiles of THCaA, DHCaA, the liquid crystalline phase and the melt to zero at 103 to 168°C, 136 to 168°C, 18 to 95°C and 18 to 115°C, respectively. Finally, a closure constraint was applied to ensure that the concentrations always sum to one, since mass balance is expected in the experiment. Thereby, the unit of the estimated concentration profiles becomes the molar fraction. The resulting MCR model, obtained after 11 iterations of the alternating least-squares algorithm and describing 98.2% of the variance in the data matrix, provides a realistic and consistent interpretation of the dehydration behavior (Fig. 8).

The practically important result from MCR is the plot of estimated concentration profiles over the temperature range (Fig. 8). This illustrates how the encountered phases

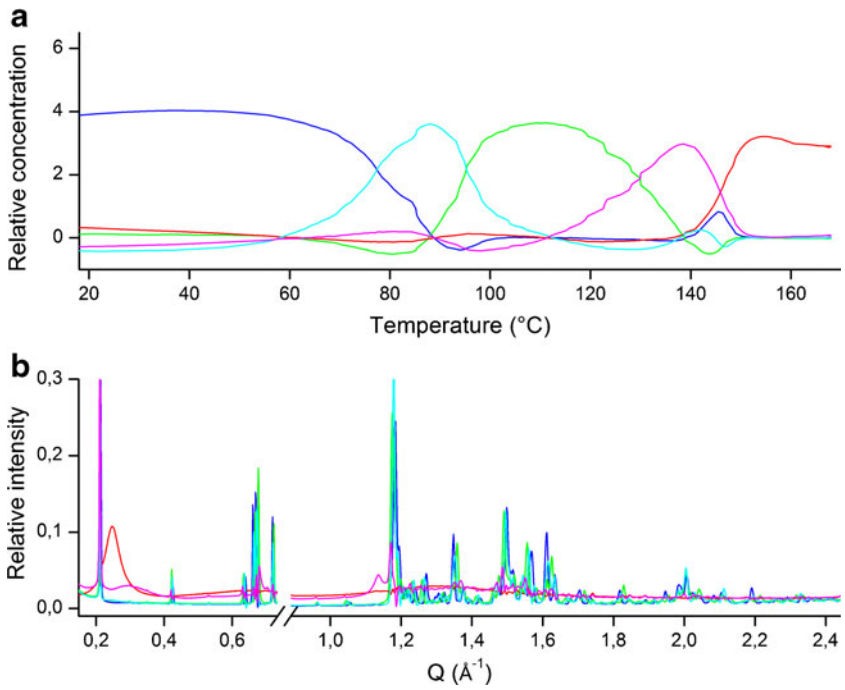


**Fig. 7** (**a**) MCR-estimated concentration profiles and (**b**) MCR-estimated XRPD patterns of pure phases encountered during dehydration and melting of the trihydrate phase of the calcium salt of atorvastatin (THCaA). No constraints were applied on the alternating least squares algorithm. Key: THCaA (*blue*), DHCaA (*cyan*), MHCaA (*green*), liquid crystalline phase (*magenta*) and melt (*red*).

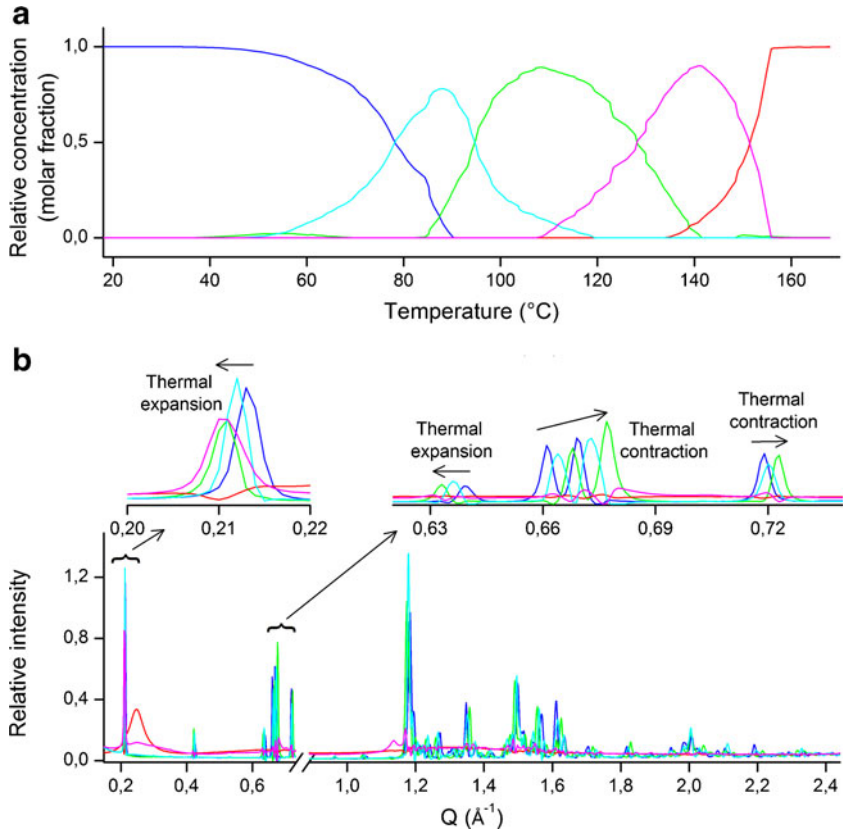


**Fig. 8** (**a**) MCR-estimated concentration profiles and (**b**) MCR-estimated XRPD diffraction patterns of pure phases encountered during dehydration and melting of the trihydrate phase of the calcium salt of atorvastatin (THCaA). The alternating least-squares algorithm was constrained to non-negativity on estimated concentration and signal profiles, and equality constraints were used to guide the predicted concentration profiles of THCaA (*blue*), DHCaA (*cyan*), the liquid crystalline phase (*magenta*) and the melt (*red*) to zero at 103 to 168°C, 136 to 168°C, 18 to 95°C and 18 to 115°C, respectively. MHCaA (*green*) was not subjected to equality constraint. Finally, a closure constraint was applied to make the concentrations sum to one.

interconvert during heating and how mixtures of phases are encountered in some temperature intervals. As a "by-product", MCR also provides estimates for the diffraction patterns of the pure component phases. Considering the SAXS region, where the peaks can be clearly resolved, the values of d(001), d(010) and d(011) derived from these estimated patterns are consistent with the plotted trends: essentially, the trihydrate corresponds to the low-temperature asymptote, the monohydrate corresponds to the high-temperature asymptote, and the dihydrate lies at the inflection point of the sigmoidal curve (Fig. 6). The estimated XRPD patterns of pure phases are thus useful indicators for structural understanding of the dehydration behavior. From a practical viewpoint, it should be stressed that these indicators emerge immediately and automatically from the MCR analysis, while the plots in Fig. 6 were derived by individual assessment of the peak positions in each of the 100 XRPD patterns. Thus, the obtained results illustrate that MCR is a convenient and apparently reliable tool for fast quantitative and qualitative assessment of phase transformations studied by X-ray powder diffraction.

## Hot-Stage Raman Spectroscopy

Hot-stage Raman spectral data were collected during heating of THCaA from 25°C to 170°C at 1°C/min (Fig. 9). Multiple subtle peak changes, including peak broadening, are observed as the temperature increases from 25°C to 155°C, and the baseline increases strongly after 160°C, which may be due to increased elastic backscattering (Rayleigh scattering) and loss of long-range order in the melt, respectively. Moreover, hot objects emit electromagnetic

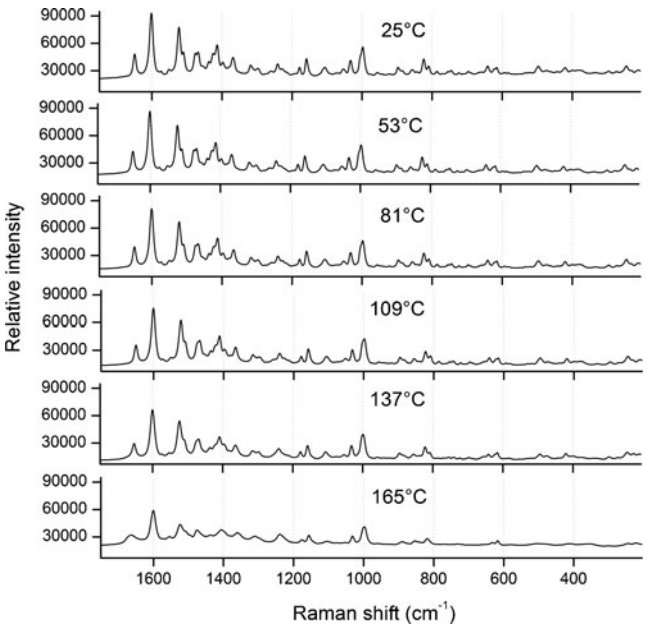


**Fig. 9** Representative Raman spectra collected during dehydration and melting the trihydrate phase of the calcium salt of atorvastatin (THCaA).

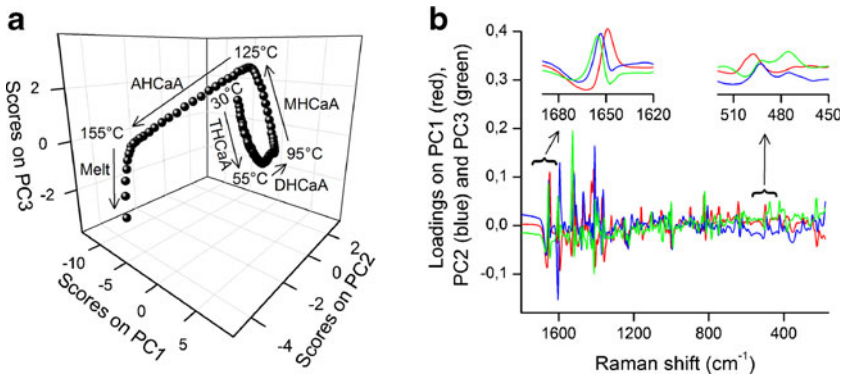


**Fig. 10** Principal component analysis (PCA) of 140 SNV transformed hot-stage Raman spectra collected during dehydration and melting of the trihydrate phase of the calcium salt of atorvastatin (THCaA) from 25 to 165°C. (**a**) Scores plot and (**b**) loadings plot of principal component 1 (PC1, 83% variance explained), principal component 2 (PC2, 12%) and principal component 3 (PC3, 4%).

radiation (*i.e.* black body radiation), which might also affect the intensity of the collected Raman spectra (32).

99% of the variation in the hot-stage Raman data collected during dehydration and melting of THCaA can be described by 3 principal components, and the spectral data is seen to cluster into four groups around 55, 95, 125 and 155°C in the scores plot, corresponding to the phase transformations of the three dehydrations (THCaA-to-DHCaA, DHCaA-to-MHCaA and MHCaA-to-liquid crystal) and the melting point of the liquid crystalline phase, respectively (Fig. 10). The PCA loadings plot indicate that PC1 describes peak shifts and peak broadening in the collected Raman spectra, while PC2 and PC3 are both affected by baseline and peak shifts. These results illustrate that Raman spectroscopy combined with principal component analysis is responsive to all phases encountered during dehydration and melting of THCaA, and the estimated transition temperatures are consistent with the VT-XRPD and TGA data. Accordingly, Raman spectroscopy may potentially be applied for solid phase monitoring of hydrate-forming drugs in pharmaceutical manufacturing environments where drug formulations are exposed to elevated temperatures.

## CONCLUSION

This study demonstrates that multivariate curve resolution (MCR) is a powerful tool for decomposing variable-temperature X-ray powder diffraction (VT-XRPD) data matrices into MCR-estimated diffraction patterns and MCR-estimated concentration profiles of pure phases of the drug salt encountered during dehydration and melting. By these means, the trihydrate phase of the calcium salt of atorvastatin (THCaA) was found to dehydrate sequentially into two partially dehydrated hydrate structures, upon heating from 25 to 110°C, with no associated breakage of the original crystal lattice. During heating from 110 to 140°C, the remaining water was lost from the solid drug salt, which instantly collapsed into a liquid crystalline phase, and an isotropic melt was formed above 155°C. To the best of our knowledge, this is the first report on a liquid crystalline phase of the calcium salt of atorvastatin. Lastly, hot-stage Raman spectroscopy and principal component analysis (PCA) was shown to provide consistent results, which confirms that Raman spectroscopy and multivariate data analysis are excellent tools for effective and inexpensive in-process monitoring of the solid phase composition of drug compounds in pharmaceutical manufacturing environments.

## ACKNOWLEDGMENTS AND DISCLOSURES

Use of the Advanced Photon Source was supported by the U. S. Department of Energy, Office of Science, Office of Basic Energy Sciences, under Contract No. DE-AC02-06CH11357. Dr. Byeongdu Lee and Dr. Xiaobing Zuo (12-ID-B beamline, Advanced Photon Source, Argonne, IL) are acknowledged for their help with the XRPD experiments. Dr. José Manuel Amigo Rubio and Dr. Jacco van de Streek (University of Copenhagen, Copenhagen, Denmark) are acknowledged for valuable discussions regarding multivariate curve resolution and X-ray powder diffraction, respectively. The PhD fellowship of N. P. A. C. was supported by Drug Research Academy (Copenhagen, Denmark), Danish Agency for Science, Technology and Innovation (Copenhagen, Denmark) and Nycomed: A Takeda Company (Roskilde, Denmark). B. V. E. is a Postdoctoral Researcher of the "Fonds voor Wetenschappelijk Onderzoek," Flanders, Belgium. N.N. was supported by a research fellowship from the United States Pharmacopeia.

## REFERENCES

1. Gardner CR, Walsh CT, Almarsson O. Drugs as materials: valuing physical form in drug discovery. Nat Rev Drug Discov. 2004;3:926–34.
2. Murphy D, Rodriguez-Cintron F, Langevin B, Kelly RC, Rodriguez-Hornedo N. Solution-mediated phase transformation of anhydrous to dihydrate carbamazepine and the effect of lattice disorder. Int J Pharm. 2002;246:121–34.
3. Wöstheinrich K, Schmidt PC. Polymorphic changes of thiamine hydrochloride during granulation and tableting. Drug Dev Ind Pharm. 2001;27:481–9.

4. Zhang GG, Law D, Schmitt EA, Qiu Y. Phase transformation considerations during process development and manufacture of solid oral dosage forms. Adv Drug Deliv Rev. 2004;56:371–90.
5. Jørgensen A, Rantanen J, Karjalainen M, Khriachtchev L, Räsänen E, Yliruusi J. Hydrate formation during wet granulation studied by spectroscopic methods and multivariate analysis. Pharm Res. 2002;19:1285–91.
6. Kogermann K, Aaltonen J, Strachan CJ, Pollanen K, Veski P, Heinamaki J, *et al.* Qualitative *in situ* analysis of multiple solid-state forms using spectroscopy and partial least squares discriminant modeling. J Pharm Sci. 2007;96:1802–20.
7. Stephenson GA, Groleau EG, Kleemann RL, Xu W, Rigsbee DR. Formation of isomorphic desolvates: creating a molecular vacuum. J Pharm Sci. 1998;87:536–42.
8. Zeitler JA, Kogermann K, Rantanen J, Rades T, Taday PF, Pepper M, *et al.* Drug hydrate systems and dehydration processes studied by terahertz pulsed spectroscopy. Int J Pharm. 2007;334:78–84.
9. Sheng J, Venkatesh GM, Duddu SP, Grant DJ. Dehydration behavior of eprosartan mesylate dihydrate. J Pharm Sci. 1999;88:1021–9.
10. Dong Z, Salsbury JS, Zhou D, Munson EJ, Schroeder SA, Prakash I, *et al.* Dehydration kinetics of neotame monohydrate. J Pharm Sci. 2002;91:1423–31.
11. Koradia V. H.L.de Diego, M.R. Elema, and J. Rantanen. Integrated approach to study the dehydration kinetics of nitrofurantoin monohydrate. J Pharm Sci. 2010;99:3966–76.
12. Rastogi S, Zakrzewski M, Suryanarayanan R. Investigation of solid-state reactions using variable temperature X-ray powder diffractrometry. I. Aspartame hemihydrate. Pharm Res. 2001;18:267–73.
13. Kogermann K, Aaltonen J, Strachan CJ, Pöllänen K, Heinämäki J, Yliruusi J, *et al.* Establishing quantitative in-line analysis of multiple solid-state transformations during dehydration. J Pharm Sci. 2008;97:4983–99.
14. Jørgensen AC, Miroshnyk I, Karjalainen M, Jouppila K, Siiria S, Antikainen O, *et al.* Multivariate data analysis as a fast tool in evaluation of solid state phenomena. J Pharm Sci. 2006;95:906–16.
15. Varmuza K and Filzmoser P. Principal component analysis. In Introduction to multivariate statistical analysis in chemometrics, CRC press, 2008, pp. 59–102.
16. de Juan A, Tauler R. Multivariate curve resolution (MCR) from 2000: Progress in concepts and applications. Crit Rev Anal Chem. 2006;36:163–76.
17. Schoonover JR, Marx R, Zhang SL. Multivariate curve resolution in the analysis of vibrational spectroscopy data files. Appl Spectrosc. 2003;57:154A–70A.
18. Kwok K, Taylor LS. Analysis of counterfeit Cialis((R)) tablets using Raman microscopy and multivariate curve resolution. J Pharm Biomed Anal. 2012;66:126–35.
19. Amigo JM, Ravn C. Direct quantification and distribution assessment of major and minor components in pharmaceutical tablets by NIR-chemical imaging. Eur J Pharm Sci. 2009;37:76–82.
20. Antonio SG, Benini FR, Ferreira FF, Rosa PCP, Paiva-Santos CD. Synchrotron X-ray powder diffraction data of atorvastatin. Powder Diffract. 2008;23:350–5.
21. Pawley GS. Unit-Cell Refinement from Powder Diffraction Scans. J Appl Crystallogr. 1981;14:357–61.
22. De Beer T, Burggraeve A, Fonteyne M, Saerens L, Remon JP, Vervaet C. Near infrared and Raman spectroscopy for the in-process monitoring of pharmaceutical production processes. Int J Pharm. 2011;417:32–47.
23. Sonje VM, Kumar L, Meena CL, Kohli G, Puri V, Jain R, *et al.* Atorvastatin calcium. Profiles Drug Subst Excip Relat Methodol. 2010;35:1–70.
24. Rinnan Å, van den Berg F, Engelsen SB. Review of the most common pre-processing techniques for near-infrared spectra. Trends Anal Chem. 2009;28:1201–22.
25. Jaumot J, Gargallo R, de Juan A, Tauler R. A graphical user-friendly interface for MCR-ALS: a new tool for multivariate curve resolution in MATLAB. Chemom Intell Lab Syst. 2005;76:101–10.
26. Atassi F, Byrn SR. General trends in the desolvation behavior of calcium salts. Pharm Res. 2006;23:2405–12.
27. Terakita A, Byrn SR. Structure and physical stability of hydrates and thermotropic mesophase of calcium benzoate. J Pharm Sci. 2006;95:1162–72.
28. Patterson J, Bary A, Rades T. Physical stability and solubility of the thermotropic mesophase of fenoprofen calcium as pure drug and in a tablet formulation. Int J Pharm. 2002;247:147–57.
29. Rades T, Müller-Goymann CC. Structural investigations on the liquid crystalline phases of fenoprofen. Pharm Pharmacol Lett. 1992;2:131–4.
30. Bunjes H, Rades T. Thermotropic liquid crystalline drugs. J Pharm Pharmacol. 2005;57:807–16.
31. Chang R. Liquid crystals. In: McGuire A, editor. Physical chemistry for the chemical and biological sciences. Sausalito: University Science Books; 2000. p. 883–8.
32. Harris DC. Spectrometers. In Quantitative Chemical Analysis. New York: W. H. Freeman and Company; 2003. p. 461–93.